



Simulation approach to electron transport phenomenon in graphene

Azeez Abdullah Barzinjy ^{a,b,*}

^a Scientific Research Center, Soran University, Kurdistan Region, Iraq

^b Physics Education Department, Faculty of Education, Tishk International University, Erbil, Iraq

ARTICLE INFO

Keywords:

Electron transport
Graphene
Quantum Hall effect
Tight-binding model
Dispersion relation
2D crystals

ABSTRACT

This investigation was originally designed to verify that the tight-binding approach utilizes an amalgamation of estimated wave functions to compute the electrical band structure. Utilizing computational tools has become essential, especially for challenging and dull problems in physics. Computer programs, in general, once utilized in the approved manner, allow physical problems to be solved and explained rapidly and efficiently at the same time. The case then is to comprehend how to swap from the abstract equations to the computer program, *i.e.*, codes. In this research, valid and numerical strategies are utilized to examine the electrical characteristics of 2D crystals through fluctuating geometries and magnetic fields. Certainty in the mathematical model is based upon those assessments of the two procedures utilizing the dispersal relationship and density of states. The numerical strategies become the importance as the examined systems goes into more complex to be investigated precisely. Throughout this study, it is confirmed that the tight-binding model utilizes a superposition of estimated wave functions to estimate the electrical band structure. This model was showed to a four-sided network and a hexagonal network to confirm the characteristics of electrons as they move over the graphene network. Particularly, this setup provides a way of investigating energy-reliant transport in graphene. The outcomes of this investigation are significant since the energy dependance of transport in mesoscopic graphene is the core of numerous odd transportation occurrences. Also, the conductance for the four-sided framework is considered utilizing the mathematical approaches and shows the accurate appearances for the quantum Hall effect.

1. Introduction

Before 85 years, Landau and Peirls have claimed that two-dimensional (2D) crystals are thermally unsteady and have zero potential for existence [1]. Their theory indicated that the varying involvement of thermal oscillations to low-dimensional crystal lattices should result in the displacement of atoms such that they turn out to be equivalent to interatomic spaces at any predictable temperatures [2]. This dispute was after that expanded by Mermin [3] and is intensely maintained by a entire body of empirical interpretations. Certainly, the melting point of thin films quickly reduces by means of reducing width, and they convert unsteady, isolate into isles or decay, at a width of, characteristically, lots of infinitesimal layers [4]. Consequently, atomic monolayers have up to now been recognized only like a fundamental part of superior 3D constructions, typically grown epitaxially on highest point of mono-crystals with corresponding crystal lattices [5]. Deprived of such a 3D base, 2D resources were might be not available till 2004, when the shared knowledge was exhibited through the investigational

detection of graphene and additional free standup 2D atomic crystals, for instance, sole layer boron nitride in addition quasi layer BSCCO [6]. It is possible to obtain these crystals on non-crystalline substrates, in liquid interruption and as deferred films [7].

Significantly, the 2D crystals were initiated not only to be incessant but also to display extraordinary crystal feature [8]. The final is very clear for the instance of graphene, wherein charge transferors can move big interatomic spaces deprived of fluctuation [9]. Through the advantage of reflection, the presence of such one atom thickness crystals might be resigned through model. Certainly, it might be claimed that the attained 2D crystallites are reduced in a semi stable state since they are removed from 3D supplies, while their tiny size (much smaller than 1 mm) and sturdy interatomic bonds promise that thermal variations cannot cause the production of displacements or additional crystal imperfections even at higher temperatures [10].

Graphene is a 2D semiconductor with a zero-width band gap. The Graphene story starts with appearance of the essential constructing block for accepting quantum systems [11,12]. Thus, due to the

* Scientific Research Center, Soran University, Kurdistan Region, Iraq.

E-mail address: azeez.azeez@soran.edu.iq.

<https://doi.org/10.1016/j.hybadv.2023.100089>

Received 30 July 2023; Received in revised form 25 August 2023; Accepted 16 September 2023

Available online 17 September 2023

2773-207X/© 2023 The Author. Published by Elsevier B.V. This is an open access article under the CC BY-NC-ND license (<http://creativecommons.org/licenses/by-nc-nd/4.0/>).

considerably good optical and electrical properties, graphene is known to hold a great promising potential in photoelectric devices, such as photodetectors, modulators, perfect absorbers, photovoltaics, photocatalysts [13–16].

The Schrödinger equation was entirely expressed by Erwin Schrödinger in 1926, and was interested by the wave performance of material subdivisions [17]. The equation takings on binary arrangements, time-dependent and time-independent. In what manner Schrödinger initially generated the time-dependent arrangement is unknown nevertheless it can effortlessly be verified utilizing the traditional wave equation and linking momentum with the De Broglie wavelength.

In the nonappearance of superiority graphene-wafers, most investigational researchers are, at present time, utilizing models acquired by micromechanical cleavage of bulky graphite, the equivalent method that permissible the separation of graphene for the earliest period [18]. Later acceptable fine-tuning, the procedure now offers great score graphene crystallites bigger than 100 μm in dimension, which is appropriate for the greatest number of investigation dedications (Fig. 1).

Cursorily, the method appearances as nonentity more refined than representation by a part of graphite or its repetitive flaking with glue tape till the tinniest bits are created [20]. A comparable method was exasperated by many groups [21,22] but merely graphite fragments 20–100 layers thickness were initiated. The issue is that the residual graphene crystallites on a substrate are enormously infrequent and concealed in a “haystack” of bulky thickness (graphite) fragments. Thus, despite the fact one were purposely looking for graphene through utilizing up-to-date procedures for reviewing atomically tinny ingredients, it might be challenging to catch those quite a few micron-size crystallites distributed in excess of, characteristically, a 1 cm^2 zone. For instance, scanning probe microscope has very low quality to examine graphene, however scanning electron microscopy, SEM, is inappropriate owing to the nonappearance of strong autographs for the amount of microscopic layers [23,24]. The acute element for achievement was the statement that graphene turns out to be noticeable in an optical microscope if located on the highest point of a Si wafer with a sensibly selected width of silicon dioxide, SiO_2 , due to a weak interloping like difference regarding an unfilled wafer [25]. If not for this modest yet operative method to probe substrates in exploration of graphene crystallites, they might possibly stay unexposed nowadays. Certainly, even having knowledge about the precise procedure, it needs distinct maintenance and persistence to discover graphene. For instance, merely a 5% dissimilarity in SiO_2 thickness, *i.e.* 315 nm rather than the existing

regular of ~ 300 nm, can cause solitary layer graphene totally imperceptible [26]. Serious assortment of the original graphite material, with the intention of having biggest conceivable grains, and the usage of recently sliced and prepared faces of graphite and SiO_2 can likewise create the entire modification. As stated by Ferrari and Basko [27] graphene possesses a perfect signal in Raman spectroscopy, which makes this procedure valuable for rapid thickness examination, although potential crystallites until now must be initially alarmed for in an optical microscope. Mohamed et al. [28] have investigated the ability of the lattice-point interaction to create lattice-point non-local correlations under the effects of the band parameter, intravalley scattering processes, and the wave numbers.

The Schrödinger equation utilizes the conservation of energy to label a remote scheme, exactly comparable to the classical mechanics. The exclusion is that we label the testify with wave functions similarly identified as the quantum states, besides the arithmetic is ruled through indicators. The wave functions comprise as considerable information of a system that we can recognise. It can be utilized to catch the probability of captivating a capacity for a physical assessment such as the location. The wave functions are utilized to just about describing non-relativistic quantum mechanical schemes precisely; for instance, the energies of specific conditions comprising subdivisions similar to electrons, protons, atoms, and molecules [29].

In this study, a fundamental electronic property of 2D graphene with the importance on density and temperature-dependent carrier transport is provided. A noticeable feature of this study is a valid and numerical strategies are utilized to examine the electrical characteristics of 2D crystals through fluctuating geometries and magnetic fields. Inevitability in the mathematical model is relying upon those assessments of the two procedures utilizing the dispersal relationship and density of states. Theoretical, quantum and semiclassical transport, are discussed in a synergistic manner in order to provide a unified and comprehensive perspective. Although the emphasis of this study is on those aspects of electron transport in graphene, other related aspects are discussed as well. Various physical mechanisms controlling transport are described in depth including quantum Hall effects, and other phenomena. This investigation is significant due to the numerous potential applications of graphene such as; lightweight, thin, and flexible electric/photonic circuits, solar cells, and various medical, chemical and industrial processes enhanced or enabled by the use of new graphene materials.

2. Theory

Frequently, the Schrödinger equation is presented in undergraduate studies where scholars initially acquire how to utilize it with the subdivision in a box [30]. Those scholars then growth on to investigate the harmonic oscillator and the Hydrogen atom, originating the wave functions and utilizing them to achieve the energies of the schemes. The time-dependent Schrödinger equation is assumed as:

$$i\hbar \frac{\partial}{\partial t} \Psi = \hat{H} \Psi, \quad (1)$$

where

$$i\hbar \frac{\partial}{\partial t} \Psi(r, t) = \left[\frac{-\hbar^2}{2m} \nabla^2 + V(r, t) \right] \Psi(r, t) \quad (2)$$

Where, the sign i is the imaginary component, \hbar is the reduced Planck constant, Ψ is the wave function, \hat{H} is the Hamiltonian operator, V is the potential energy and ∇^2 is Laplacian operator. The term $\frac{-\hbar^2}{2m} \nabla^2$ is the dynamic energy part and can be expressed by means of $\frac{\hat{p}^2}{2m}$. $V(r, t)$ signifies the potential interrelating by way of the particle and relies upon together location and time. The summation of the twofold relations is the Hamiltonian and might be expressed as an operative \hat{H} , the entire energy operative. $\Psi(r, t)$ is the wave function of the particle [31].

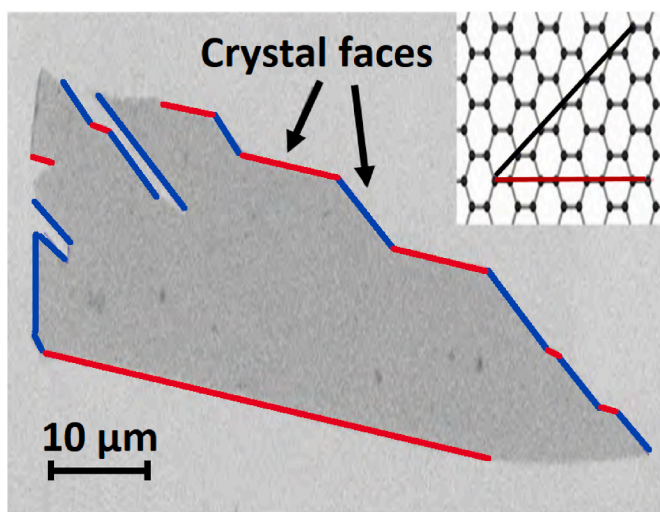


Fig. 1. Scanning Electron Microscopy image of a bulky graphene crystal, showing that the majority of the crystal faces are wavy and wingchair ends as specified by red and blue lines and demonstrated in the enclosure [19].

There are two arrangements of the Schrödinger formula, the time-dependent as designated beyond and time-independent arrangement. The time-independent arrangement inscribed straight underneath suggests that for a Hamiltonian there is a precise energy accompanying through the scheme, and for that specific energy there is a wave function related to it [32]. The wave-function for this kind of Schrödinger formula relies merely upon the location of the particle. The explanations for the time-independent Schrödinger formula are standing-waves [33].

$$E\Psi = \hat{H}\Psi \quad (3)$$

$$E\Psi(r) = \left[\frac{-\hbar^2}{2m} \nabla^2 + V(r) \right] \Psi(r) \quad (4)$$

Where E is the total energy. The Schrödinger equation is accomplished of observing at extra stimulating systems than only distinct particle schemes. To this finale replica have been prepared to excerpt evidence regarding quantum systems, for instance demonstrating the performance of electrons as they move over crystals. The evidence collected from these replicas is the electric band construction, or the varieties of energies that the electrons in the crystal might possess. A characteristic prototypical for observing at these types of schemes is the Tight-Binding exemplary [34].

2.1. Tight-binding model

The tight-binding exemplary is utilized to model an electron in a periodic potential [35]. The exemplary twitches with the supposition that the electron is firmly inevitable to the atomic location. This permits the usage of a direct arrangement of atomic orbitals to signify the wave-function of the scheme, a mixing of atomic wave functions. Functioning with periodic potentials, a Bloch wave-function is utilized to adapt the atomic wave functions, providing transform regularity to the wave functions. The tight-binding prototypical provides a simple-minded yet extremely convenient method to exemplify the band construction for numerous resources [36].

The tight binding construction of group electrons might also be employed extremely simple in the additional quantization verbal and offers a relatively instinctive clarification. In the logical common sense, the tight binding model is a distinct, network, form of the uninterrupted Schrödinger equation, consequently it is regularly utilized in arithmetical intentions. With the intention of generate a modest Hamiltonian to designate a 1D scheme, an supposition is prepared that the electrons are firmly destined to its lattice location deprived of dealings or bounding, with an on-site energy ϵ [37].

It is informative for additional search the 1D sequence then determines its dispersal relationship, otherwise in what manner the energy alters against the momentum wave-vector. It is forthright to compute through straight replacement of the Fourier sequences into the formation and annihilation operatives [38]:

$$H = \epsilon - t \left[e^{ik(a_x)} + e^{-ik(a_x)} \right] \quad (5)$$

Then,

$$E_k = \epsilon - 2t[\cos(k_x a)] \quad (6)$$

$$\text{Where } k_x = 2\pi n/Na \quad (7)$$

Where ϵ the location energy, t is the hopping integral, k is the wave number, a is lattice vector and a_x is the Fourier coefficients parameter.

Fig. 2 shows the dispersal relationship a 1D sequence by means of the precise explanation found over the replacement of the Fourier illustration of the annihilation and formation operative.

It is significant to observe that if the on-site energy differs, a dissimilar technique needs to be utilized to discover an explanation of the Hamiltonian. To state this concern, a computational technique that utilizes an precise diagonalization process is essential to resolve for the

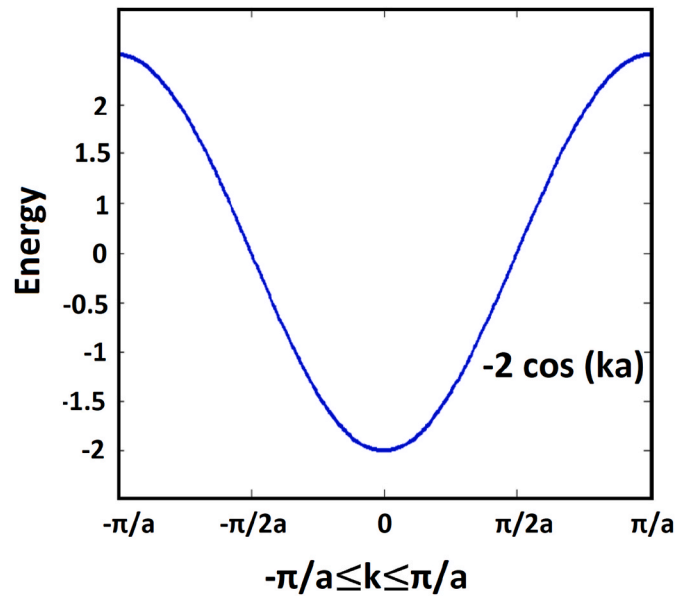


Fig. 2. Dispersal relationship for a 1D sequence utilizing the precise solution acquired over the replacement of the Fourier illustration of the annihilation and formation operative.

schemes' eigenvalues [39]. This is a communal method utilized in complex schemes.

This is only an example of what might be done with this technique [40]. After that, the prototypical can be extended to switch a 2D scheme with divergent geometries, manifold lattice schemes, presence of an unchanging magnetic field, and conductance controls [41].

In order to acquire a superior impression of in what way more complex schemes are completed, the difficulty of the prototypical is progressively amplified whereas testing for correctness, or the accuracy of the consequences they create in relation to an investigative method. In the 2D model, binary diverse approaches might be verified for explaining the similar scheme: one is utilizing a logical method, and an additional utilizing a computational technique [42].

One can rise the intricacy of the prototypical through growing the sizes of the prototypical and protecting the geometry as easy as conceivable; for this purpose, a four-sided lattice was selected. The four-sided lattice comprises N_x times N_y number of atomic places alongside the x as well as y directions. The Hamiltonian for this prototypical deliver as:

$$H = \sum_{ij} \epsilon_{ij} A_{ij}^\dagger A_{ij} - t \sum_{ij} \left(A_{i+1,j}^\dagger A_{ij} + A_{i,j+1}^\dagger A_{ij} + h.c. \right) \quad (8)$$

ϵ_{ij} is the location energy of an electron at the ij th atom and it is associated with the complaint of the scheme, in which for straightforwardness is fixed on zero otherwise a continuous. In the overhead formula, t is the springing energy amongst the neighboring locations in both the i th or the j th route. At this point, $A_{ij}^\dagger A_{ij}$ are the formation and obliteration parameters, that generate or abolish the residence of the electron over the ij th site. Once more, the formation and obliteration parameters are signified as their Fourier transforms through suitable subscripts [43]:

$$A_{ij} = \frac{1}{\sqrt{N}} \sum_k A_k e^{i\vec{k} \cdot \vec{R}_{ij}} \quad (9)$$

$$A_{ij}^\dagger = \frac{1}{\sqrt{N}} \sum_k A_k^\dagger e^{-i\vec{k} \cdot \vec{R}_{ij}} \quad (10)$$

In this equation, the expressions \vec{k} and \vec{R}_{ij} are the wave-vector as well

as frame vectors, correspondingly. They are delicate to the geometry of the lattice and need to be sensibly measured for once relieving and adding above i and j :

$$E = \frac{1}{N} \sum_{i,j,k} \epsilon_{ij} A_k^\dagger A_k e^{-i\vec{k} \cdot \vec{R}_{ij}} e^{i\vec{k} \cdot \vec{R}_{ij}} - \frac{t}{N} \sum_{i,j,k} \left(A_k^\dagger e^{-i\vec{k} \cdot \vec{R}_{i+1,j}} A_k e^{i\vec{k} \cdot \vec{R}_{i,j}} + A_k^\dagger e^{-i\vec{k} \cdot \vec{R}_{i,j+1}} A_k e^{i\vec{k} \cdot \vec{R}_{i,j}} + h.c. \right) \tag{11}$$

$$E = \frac{1}{N} \sum_{i,j,k} \epsilon_{ij} A_k^\dagger A_k e^{i(\vec{k}-\vec{k}) \cdot \vec{R}_{ij}} - \frac{t}{N} \sum_{i,j,k} \left(A_k^\dagger A_k \left(e^{i(\vec{k}-\vec{k}) \cdot \vec{R}_{ij}} e^{-i\vec{k} \cdot \vec{R}_i} + e^{i(\vec{k}-\vec{k}) \cdot \vec{R}_{ij}} e^{-i\vec{k} \cdot \vec{R}_j} + h.c. \right) \right) \tag{12}$$

$$E = \epsilon \sum_k A_k^\dagger A_k - t \sum_k A_k^\dagger A_k \left(e^{i\vec{k} \cdot (-l\hat{i})} + e^{i\vec{k} \cdot (-l\hat{j})} + h.c. \right) \tag{13}$$

Wherein l is the lattice constant, and ϵ is occupied to be not changing at each location. The overhead formula shrinks to cosines once joint through the Hermitian conjugate [44]:

$$E = \epsilon - 2t \sum_k \left(\cos(k_i l) + \cos(k_j l) \right) \tag{14}$$

Equation (14) can provide the dispersion-relationship for a 2D four-sided lattice above the primary Brillouin zone. Fig. 3 displays the dispersion relationship for a 2D four-sided lattice in excess of the initial Brillouin zone. The image shows the dispersal relationship for a nearby incessant lattice. The dispersion relationship is 1D sophisticated than the momentum vector. So as to observe the dispersion-relationship for a 3D crystal, additional method to signify the dispersion-relationship is required.

2.2. Limitations of the tight-binding model

It is significant to notice that, although we utilized a simple tight-binding model taking into account only the closest neighbors, The result here is robust in contrast to any guesses about wavefunctions and is a consequence of the symmetry of graphene neglecting spin-orbital coupling.

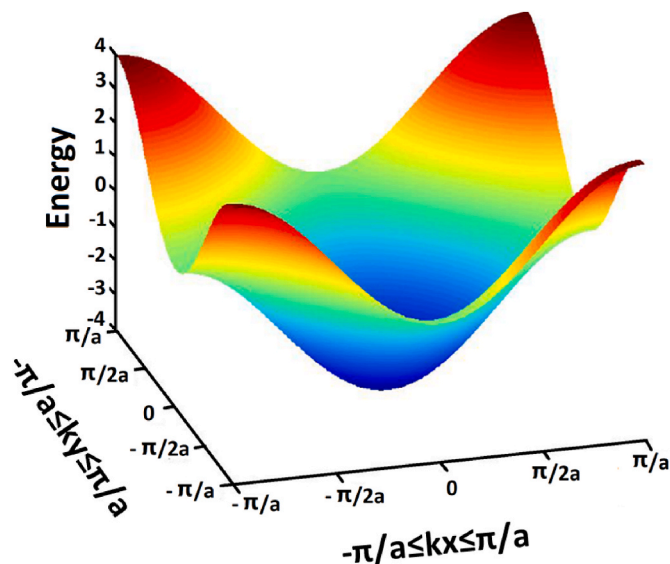


Fig. 3. Dispersion-relationship for a 2D four-sided lattice above the primary Brillouin zone.

Since tight-binding models possess insufficient electronic degrees of freedom and such a simple Hamiltonian, they can be utilized to treat much greater systems, describe the effects of disorder, and model

physical phenomena that are in accessible to first-principles electronic structure designs. However, As mentioned before the values of the matrix elements are not so large in comparison with the ionization energy because the potentials of neighboring atoms on the central atom are limited. If the matrix elements are not relatively small it means that the potential of the neighboring atom on the central atom is not small either. In that case it is an indication that the tight-binding model is not a very good model for the description of the band structure for some reason. The interatomic distances can be too small or the charges on the atoms or ions in the lattice is wrong for example.

3. Computational approaches

There is a requisite to signify the Hamiltonian in a way that a processor can employ and help in resolving for the eigenvalues. In order to organise this, the wave function of the scheme is prolonged by the wave functions of the atomic orbitals $\Psi = \sum_i c_i \varphi_{(r-R_i)}$.

3.1. Matrix approach

The characteristics of matrix procedure that states $H\psi = E\psi$ can be utilized. By means of this, the matrix might be diagonalized then resolved for the allowable energies of the scheme, or the eigenvalues. Along with resolving for the eigenvalues, the coefficients c_i might be attained, utilized after that to obtain the conductance of the scheme [45].

For example, we might study a 1D sequence of atoms, exactly like what was stated in the outline. Signified underneath is $H\psi = E\psi$ for a 1D sequence of four atoms with $\psi = \sum_i c_i \varphi_{(r-R_i)}$. Meanwhile possible connections in the Hamiltonian are not deliberated, the kinetic energy expressions are in its place studied. The onsite energies and springing energies are itemised underneath as well as they are signified with their overlay essential $= \langle \varphi(r) | H | \varphi(r) \rangle$, and $t = -\langle \varphi(r) | H | \varphi(r-a) \rangle$ in that order.

$$H\psi = \begin{pmatrix} \epsilon & -t & 0 & -t \\ -t & \epsilon & -t & 0 \\ 0 & -t & \epsilon & -t \\ -t & 0 & -t & \epsilon \end{pmatrix} \begin{pmatrix} c_1 \varphi_{(r-R_1)} \\ c_2 \varphi_{(r-R_2)} \\ c_3 \varphi_{(r-R_3)} \\ c_4 \varphi_{(r-R_4)} \end{pmatrix} = E\psi \tag{15}$$

In equation (15), one can transfer E to the additional lateral of the equation and resolve the determinate $\det[H - E I] \psi = 0$, wherein, once resolved, attains the allowable energies of the scheme and the quantities to the wave function.

On-going with a novel instance, a 2D scheme might be examined, determining the logical consequences and likening them through the arithmetical outcomes. For this, formula (14) might be utilized to generate a list of eigenvalues and associate them to the arithmetical outcomes produced by formula (15).

Think over a 3×3 square matrix of atoms with adjacent neighbour bounding connections and no onsite energy. To confirm that the eigenvalues are precise, there is a requisite to discretize formula (14) and resolve for entire of the distinct energies. Recalling that the borderline circumstances cause distinct momentum $k_i = \frac{2\pi n}{aN_i}$, can be utilized to

Nearest neighbour vectors : $\delta_1 = a\left(-\frac{1}{2}, -\frac{\sqrt{3}}{2}\right), \delta_2 = a(1, 0), \delta_3 = a\left(-\frac{1}{2}, \frac{\sqrt{3}}{2}\right)$

$$A_{i,j} = \frac{1}{\sqrt{N}} \sum_k A_k e^{i\vec{k} \cdot \vec{R}_{i,j}}, A_{i,j}^\dagger = \frac{1}{\sqrt{N}} \sum_k A_k e^{-i\vec{k} \cdot \vec{R}_{i,j}}, B_{i,j}^\dagger = \frac{1}{\sqrt{N}} \sum_k B_k^\dagger e^{-i\vec{k} \cdot \vec{R}_{i,j}}, B_{i,j} = \frac{1}{\sqrt{N}} \sum_k B_k^\dagger e^{i\vec{k} \cdot \vec{R}_{i,j}}$$

Disregarding on situate energies for straightforwardness, the Fourier transforms of the formation and obliteration operatives are relieved obsessed by the Hamiltonian:

$$H = \frac{-t}{N} \sum_{\langle i,j,k \rangle} \left(A_k^\dagger e^{-i\vec{k} \cdot \vec{R}_{i,j+\delta_1}} B_k e^{i\vec{k} \cdot \vec{R}_{i,j}} + A_k^\dagger e^{-i\vec{k} \cdot \vec{R}_{i,j+\delta_2}} B_k e^{i\vec{k} \cdot \vec{R}_{i,j}} + A_k^\dagger e^{-i\vec{k} \cdot \vec{R}_{i,j+\delta_3}} B_k e^{i\vec{k} \cdot \vec{R}_{i,j}} + h.c. \right) \tag{21}$$

$$H = \frac{-t}{N} \sum_{\langle i,j,k \rangle} \left[\left(e^{i(\vec{k}-\vec{k}') \cdot \vec{R}_{i,j}} e^{-i\vec{k}' \cdot \delta_1} + e^{i(\vec{k}-\vec{k}') \cdot \vec{R}_{i,j}} e^{-i\vec{k}' \cdot \delta_2} + e^{-i(\vec{k}-\vec{k}') \cdot \vec{R}_{i,j}} e^{-i\vec{k}' \cdot \delta_3} \right) A_k^\dagger B_{k'} + h.c. \right] \tag{22}$$

Here $\sum_{ij} e^{i(\vec{k}-\vec{k}') \cdot \vec{R}_{i,j}} = N_i N_j \delta_{\vec{k},\vec{k}'} \delta_{k,k'}$ and $N = N_i N_j$ Upon substitution, the expression reduces to:

$$H = -t \sum_k \left(e^{-i\vec{k} \cdot \delta_1} + e^{-i\vec{k} \cdot \delta_2} + e^{-i\vec{k} \cdot \delta_3} + h.c. \right) A_k^\dagger B_k + h.c. \tag{23}$$

This Hamiltonian is not as effortlessly resolved as in the Square-lattice situation; the momentum operators are not the same, so the synopsis generates a 2×2 matrix demonstrating $A_k, B_k, A_k^\dagger, B_k^\dagger$. This is owing to the crystal possessing an A and B lattice. In order to determine the allowable energies, it is adequate to proceeds the determinate of the Hamiltonian [52]:

$$H = -t \begin{pmatrix} A_k^\dagger & B_k^\dagger \end{pmatrix} \begin{pmatrix} 0 & \sum_i e^{-i\vec{k} \cdot \delta_i} \sum_i i\vec{k} \cdot \delta_i \\ \sum_i e^{-i\vec{k} \cdot \delta_i} \sum_i i\vec{k} \cdot \delta_i & 0 \end{pmatrix} \begin{pmatrix} A_k \\ B_k \end{pmatrix} \tag{24}$$

Dispersion Relation for Graphene

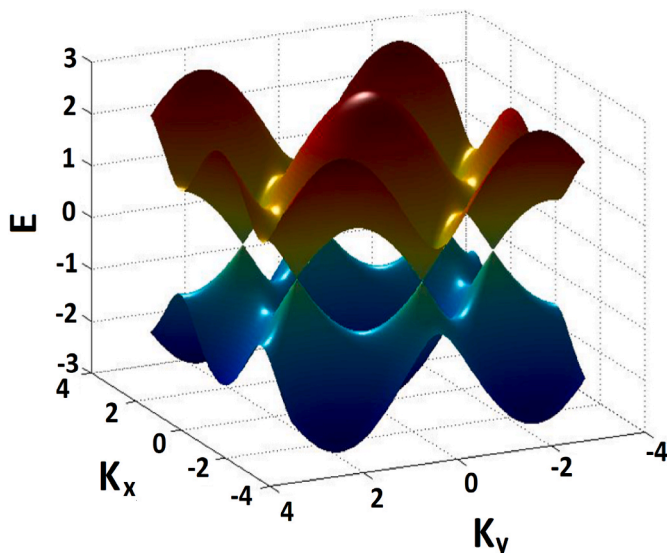


Fig. 5. The dispersion-relationship for Graphene from $-\pi$ to π in K_x and K_y .

$$\begin{vmatrix} -E \sum_i e^{-i\vec{k} \cdot \delta_i} & \\ \sum_i i\vec{k} \cdot \delta_i & -E \end{vmatrix} = 0 \tag{25}$$

$$E_k = \pm \left[3 + 2 \cos(\sqrt{3} k_y a) + 4 \cos\left(\frac{\sqrt{3}}{2} k_y a\right) \cos\left(\frac{3}{2} k_x a\right) \right]^{1/2} \tag{26}$$

Once some algebraic calculations made, the allowable energy against the momentum is initiated and presented overhead. The energy range can be plotted out precisely utilizing k_x as well as k_y . The momentum k_x then k_y are separate besides the entire number of eigenvalues relies upon

the number of atomic places in the crystal. The energy standards approximately equal to an uninterrupted function as the quantity of atomic places reaches infinity. Fig. 5 represents the dispersion-relationship for Graphene starting from $-\pi$ to π in K_x and K_y [53].

The eigenvalues of this Hamiltonian are computed arithmetically utilizing the similar technique by way of in the square-lattice instance. A Hamiltonian is built utilizing formula (20) and the eigenvalues are initiated. The eigenvalues of the binary schemes are not identical owing to in what way the standards are gotten for an individual scheme [54]. So as to associate the consequences a regularised density of states for apiece scheme is intended and overlaid. The consequences are presented in Fig. 6, which represents the density of situations for Graphene. The blue line signifies the investigative consequences of the tight-binding approach for Graphene. The red line displays the density of states for a 60×60 framework. Apiece of the density of circumstances possesses their energies discarded through energy thickness and regularised, formerly overlaid [55].

As stated formerly, graphene possesses a honeycomb 2D crystal

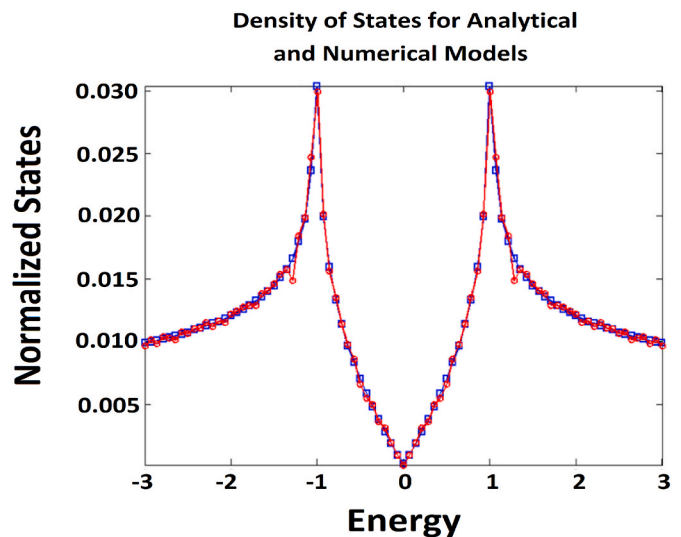


Fig. 6. Graphene density of states. The blue line signifies the investigative consequences of the tight-binding prototypical for Graphene. The red line displays the 60×60 lattice density of states.

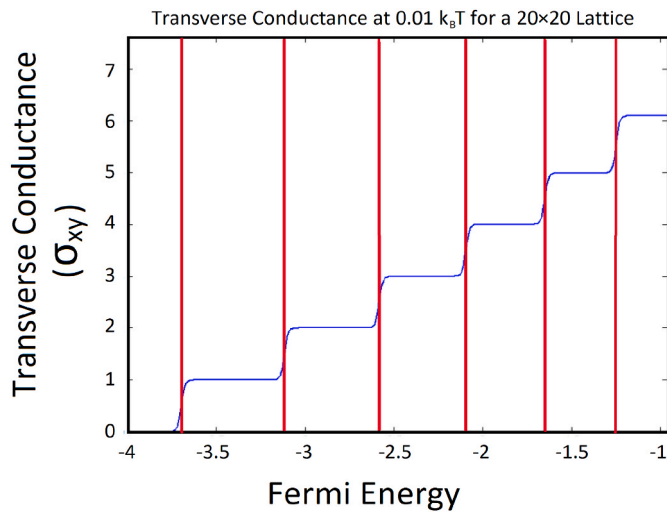


Fig. 7. Transverse conductance vs. Fermi energy, for a 20×20 crystal lattice in a uniform magnetic field.

lattice, which is composed of sp^2 crossbred carbon atoms that are close-packed and attached together with σ -bonds. The strong σ -bonds in the graphene lattice provide the high mechanical properties of graphene. Every single carbon atom has a π -orbital that creates a delocalized electrons network. The π -electrons can transfer spontaneously inside the graphene crystal plane; therefore, the graphene possesses outstanding electrical conductivity [56]. The exclusive performance of electrons in this 2D quantum system not only opens up numerous motivating questions in mesoscopic transportation in electronic systems but might, similarly, offer the basis for new carbon based electric and magnetic field effect device applications, for instance ballistic metallic/semiconducting graphene ribbon devices and electric field effective spin transference devices employing spin-polarized edge state [57].

We compute the longitudinal and transverse conductance over a change in the Fermi energy to produce a profile curve of the conductance. The Fermi energy, E_f , moves from the base of the crystal lattice's energy spectrum to the top, giving a range of -4 to 4 . At a particular temperature, magnetic field, and degree of disorder, the computation is performed. Below, the transverse conductance, which is of special interest is explained.

$$\sigma_{xy} = \frac{ie^2\hbar}{N} \sum_{\alpha} \sum_{\beta \neq \alpha} (f_{\alpha} - f_{\beta}) \frac{\langle \alpha | \hat{u}_k | \beta \rangle \langle \beta | \hat{u}_l | \alpha \rangle}{(\epsilon_{\alpha} - \epsilon_{\beta}) + \eta^2} \quad (27)$$

Here, N represents the total number of atoms or sites, f_{α} and f_{β} are the Fermi distribution for electrons at absolute temperature for states $|\alpha\rangle$ and $|\beta\rangle$, the indices k and l are x and y , The states $|\alpha\rangle$ and $|\beta\rangle$ are the Eigen states of the Hamiltonian corresponding to the Eigen energies ϵ_{α} and ϵ_{β} , respectively, e , \hbar and η are constant and \hat{u}_k and \hat{u}_l are velocity operators.

The Landau levels system are covered on the transverse conductance graph in Fig. 7. This Figure shows how Fermi energy, E_f , and landau levels relate to one another. The transverse conductivity increases by an integer amount of e^2/h , when the Fermi energy goes over the landau level and this is due to the quantum hall effect. The choice of magnetic flux affects the number of plateaus because it affects how many Landau levels there are. A 20×20 system with a flux of $2\pi/20$ and a low finite temperature of 0.1 is shown in Fig. 7. In this graph the transverse conductance, blue color, is place over the energy spectrum for a 20×20 crystal lattice in a uniform magnetic field. This graph obviously displays integer jumps in the transverse conductance for every Landau-level that the Fermi energy passes over, from the right-hand side. This is basically the quantum hall effect that has been discussed previously.

Once electrons are confined in 2D materials, quantum mechanically

improved transportation phenomena for instance the quantum Hall effect can be detected. Graphene, comprising of an isolated single-atomic layer of graphite, is a perfect comprehension of such a 2D system. Nevertheless, its behavior is anticipated to fluctuate noticeably from the well-investigated circumstance of quantum wells in conventional semiconductor crossing point. This alteration rises from the exclusive electronic properties of graphene, which displays electron-hole degeneracy and disappearing carrier mass near the point of charge neutrality. Certainly, a characteristic half-integer quantum Hall effect has been estimated hypothetically, as has the presence of a non-zero electron wavefunction. In addition to their purely scientific curiosity, these infrequent quantum transport phenomena may cause novel applications in carbon-based electronic and magneto-electronic devices.

5. Conclusion

All the way through this investigation, it has been verified that the essentials of the tight-binding approach utilize an amalgamation of estimated wave functions to compute the electrical band-structure. This approach was conducted to a four-sided lattice and a hexagonal lattice to examine the characteristics of electrons as they move over the lattices. A magnetic field is then enforced and the spectrum energy is determined, in addition to the conductance. Once a magnetic field is enforced, the energy band splits into Landau-levels. Concisely the expansion of the Landau-levels was deliberated once randomness was presented to the scheme. Once the Fermi-Energy of the four-sided lattice scheme moves over the Landau-levels, a numeral variation of e^2/h is perceived in the crosswise conductance, wherein it represents the IQHE for a square-lattice. The impact of temperature was perceived in the conductance of the four-sided lattice. Once the temperature raised, the alteration among tables in the conductance extended, besides high temperatures wash away from the tables entirely.

Ethics approval and consent to participate

Not applicable.

Human and animal rights

No humans were used for studies that are the basis of this research.

Consent for publication

Not applicable.

Availability of data

The data and supportive information is available within the article.

Funding

This research received no external funding.

Declaration of competing interest

The authors declare that they have no known competing financial interests or personal relationships that could have appeared to influence the work reported in this paper.

Acknowledgements

The author would like to acknowledge Dr Mukhtar Ahmed at SISAF, Ulster University, UK, for his valuable assistance throughout this research. He similarly wants to acknowledge Dr. David M.W. Waswa at Tishk International University-Erbil, Iraq for his industrious proof-reading of this manuscript. If someone requests the Matlab codes, please

contact the corresponding author for any supplementary assistance.

List of abbreviations

2D	two-dimensional
SEM	scanning electron microscopy
SiO ₂	silicon dioxide
DoS	density of states

References

- [1] L. Landau, Zur Theorie der phasenumwandlungen II, Phys. Z. Sowjetunion 11 (545) (1937) 26–35.
- [2] M.J. Allen, V.C. Tung, R.B. Kaner, *Honeycomb carbon: a review of graphene*. Chemical reviews 110 (1) (2010) 132–145.
- [3] N.D. Mermin, Crystalline order in two dimensions, Phys. Rev. 176 (1) (1968) 250.
- [4] T. Guin, et al., *Ultrastrong, chemically resistant reduced graphene oxide-based multilayer thin films with damage detection capability*. ACS applied materials & interfaces 8 (9) (2016) 6229–6235.
- [5] K. Kim, et al., Epitaxially grown strained pentacene thin film on graphene membrane, Small 11 (17) (2015) 2037–2043.
- [6] T. Low, et al., Polaritons in layered two-dimensional materials, Nat. Mater. 16 (2) (2017) 182–194.
- [7] S. Stankovich, et al., *Graphene-based composite materials*. nature 442 (7100) (2006) 282.
- [8] J. Qian, et al., *Solution-processed 2D molecular crystals: fabrication techniques, transistor applications, and physics*. Advanced materials technologies 4 (5) (2019) 1800182.
- [9] F. Fauzi, et al., Gas and humidity sensing with quartz crystal microbalance (QCM) coated with graphene-based materials—A mini review, Sensor Actuator Phys. (2021) 112837.
- [10] L. Landau, E. Lifshitz, *Statistical Physics, 3rd. Edition, 1*, Pergamon Press, Oxford, 1980, 1980.
- [11] M. Segal, Selling graphene by the ton, Nat. Nanotechnol. 4 (10) (2009) 612–614.
- [12] M. Segal, Material history: learning from silicon, Nature 483 (7389) (2012) S43–S44.
- [13] J. Chen, et al., Bandwidth-tunable absorption enhancement of visible and near-infrared light in monolayer graphene by localized plasmon resonances and their diffraction coupling, Results Phys. 49 (2023) 106471.
- [14] Y. Wu, et al., *Ultra-narrowband, electrically switchable, and high-efficiency absorption in monolayer graphene resulting from lattice plasmon resonance*. Results in Physics 51 (2023) 106768.
- [15] Z. Yan, et al., Ultra-broadband and completely modulated absorption enhancement of monolayer graphene in a near-infrared region, Opt Express 30 (19) (2022) 34787–34796.
- [16] J. Chen, et al., *Broadband, wide-incident-angle, and polarization-insensitive high-efficiency absorption of monolayer graphene with nearly 100% modulation depth at communication wavelength*. Results in Physics 40 (2022) 105833.
- [17] E. Schrödinger, An undulatory theory of the mechanics of atoms and molecules, Phys. Rev. 28 (6) (1926) 1049.
- [18] D. Pacilé, et al., Near-edge X-ray absorption fine-structure investigation of graphene, Phys. Rev. Lett. 101 (6) (2008) 66806.
- [19] A.K. Geim, K.S. Novoselov, The rise of graphene, Nat. Mater. 6 (3) (2007) 183.
- [20] K.S. Novoselov, et al., Electric field effect in atomically thin carbon films, science 306 (5696) (2004) 666–669.
- [21] Y. Ohashi, et al., Size effect in the in-plane electrical resistivity of very thin graphite crystals, Carbon 36 (4) (1998) 475–476.
- [22] S. Hong, et al., Design and test of a graphite target system for in-flight fragment separator, in: Nuclear Instruments and Methods in Physics Research Section A: Accelerators, Spectrometers, Detectors and Associated Equipment, vol. 752, 2014, pp. 1–5.
- [23] J. Kim, F. Kim, J. Huang, *Seeing graphene-based sheets*. Materials today 13 (3) (2010) 28–38.
- [24] S. Li, M. Liu, X. Qiu, Scanning probe microscopy of topological structure induced electronic states of graphene, Small Methods 4 (3) (2020) 1900683.
- [25] D.L. Duong, et al., Layer-controlled single-crystalline graphene film with stacking order via Cu–Si alloy formation, Nat. Nanotechnol. 15 (10) (2020) 861–867.
- [26] P. Goh, A. Ismail, *A review on inorganic membranes for desalination and wastewater treatment*. Desalination 434 (2018) 60–80.
- [27] A.C. Ferrari, D.M. Basko, Raman spectroscopy as a versatile tool for studying the properties of graphene, Nat. Nanotechnol. 8 (4) (2013) 235–246.
- [28] A.-B.A. Mohamed, et al., Non-local correlation dynamics in two-dimensional graphene, Sci. Rep. 12 (1) (2022) 1–12.
- [29] R.P. Feynman, Space-time approach to non-relativistic quantum mechanics, in: Feynman's Thesis—A New Approach to Quantum Theory, 2005, pp. 71–109.
- [30] D.J. Tannor, Introduction to Quantum Mechanics: a Time-dependent Perspective, University Science Books, 2007.
- [31] J.J. Sakurai, J. Napolitano, Modern Quantum Mechanics, Cambridge University Press, 2017.
- [32] L.D. Carr, C.W. Clark, W.P. Reinhardt, Stationary solutions of the one-dimensional nonlinear Schrödinger equation. II, Case of attractive nonlinearity. Phys. Rev. A 62 (6) (2000) 63611.
- [33] C. Sulem, P.-L. Sulem, Springer science & business media, The nonlinear Schrödinger equ.: self-focusing and wave collapse 139 (2007).
- [34] V.M. Pereira, J.L. Dos Santos, A.C. Neto, Modeling disorder in graphene, Phys. Rev. B 77 (11) (2008) 115109.
- [35] T. Liu, A Tight Binding Model for the Energetics of Hydrocarbon Fragments on Metal Surfaces, University of Minnesota, 2000.
- [36] G.-B. Liu, et al., Three-band tight-binding model for monolayers of group-VIB transition metal dichalcogenides, Phys. Rev. B 88 (8) (2013) 85433.
- [37] F. Verstraete, et al., Renormalization-group transformations on quantum states, Phys. Rev. Lett. 94 (14) (2005) 140601.
- [38] H. Bruus, K. Flensberg, Oxford university press, Many-body quant. theor. Condens. Matter Phys.: an introd (2004).
- [39] E. Polizzi, Density-matrix-based algorithm for solving eigenvalue problems, Phys. Rev. B 79 (11) (2009) 115112.
- [40] A. Kumar, P. Singh, K.B. Thapa, Study of super absorption properties of 1D graphene and dielectric photonic crystal for novel applications. Optical and Quantum Electronics 52 (10) (2020) 1–12.
- [41] Y. Zhou, et al., Tuning the dispersion relation of a plasmonic waveguide via graphene contact, EPL 107 (3) (2014) 34007.
- [42] X.-H. Hou, et al., Elastic constants and phonon dispersion relation analysis of graphene sheet with varied Poisson's ratio, Compos. B Eng. 162 (2019) 411–424.
- [43] C. Witte, Creation and Annihilation Operators, in *Compendium Of Quantum Physics*, Springer, 2009, pp. 139–145.
- [44] H. Terashima, M. Ueda, *Hermitian conjugate measurement*. Physical Review A 81 (1) (2010) 12110.
- [45] L.-M. Duan, R. Raussendorf, Efficient quantum computation with probabilistic quantum gates, Phys. Rev. Lett. 95 (8) (2005) 80503.
- [46] R. Alicandro, M. Cicalese, *A general integral representation result for continuum limits of discrete energies with superlinear growth*. SIAM journal on mathematical analysis 36 (1) (2004) 1–37.
- [47] S. Carr, et al., Derivation of Wannier orbitals and minimal-basis tight-binding Hamiltonians for twisted bilayer graphene: first-principles approach, Phys. Rev. Res. 1 (3) (2019) 33072.
- [48] H. Faßbender, et al., Hamiltonian square roots of skew-Hamiltonian matrices. Linear algebra and its applications 287 (1–3) (1999) 125–159.
- [49] F. Xie, et al., Twisted bilayer graphene. VI. An exact diagonalization study at nonzero integer filling, Phys. Rev. B 103 (20) (2021) 205416.
- [50] V.M. Pereira, et al., Disorder induced localized states in graphene, Phys. Rev. Lett. 96 (3) (2006) 36801.
- [51] J. Schrieffer, P. Wolff, Relation between the anderson and kondo Hamiltonians, in: Selected Papers of J Robert Schrieffer: in Celebration of His 70th Birthday, World Scientific, 2002, pp. 371–372.
- [52] D. Gunlycke, C.T. White, Graphene valley filter using a line defect, Phys. Rev. Lett. 106 (13) (2011) 136806.
- [53] M.I. Katsnelson, *Graphene: carbon in two dimensions*. Materials today 10 (1–2) (2007) 20–27.
- [54] D.J. Fernández, D.I. Martínez-Moreno, Bilayer graphene coherent states. The European physical journal plus 135 (9) (2020) 1–25.
- [55] S. Dröscher, et al., Quantum capacitance and density of states of graphene, Appl. Phys. Lett. 96 (15) (2010) 152104.
- [56] P. Hess, Bonding, structure, and mechanical stability of 2D materials: the predictive power of the periodic table, Nanoscale Horiz. 6 (11) (2021) 856–892.
- [57] C.L. Kane, E.J. Mele, Quantum spin Hall effect in graphene, Phys. Rev. Lett. 95 (22) (2005) 226801.